5th Conference on Production Systems and Logistics

# Assessment of a Novel Process to Enable Roll-to-roll Production of Catalyst Coated Membranes

Achim Kampker[1], Heiner Heimes[1], Mario Kehrer[1], Sebastian Hagedorn[1], Niels Hinrichs[1*], Philip Heyer[1]

[1]*Chair of Production Engineering of E-Mobility Components (PEM) of RWTH Aachen University, Bohr 12, 52072 Aachen, Germany*
**Corresponding Author*

**Abstract**

Hydrogen is becoming an increasingly important energy carrier within the next few years for different applications within different industries, such as chemical industry, steel production or mobility. Furthermore, it can be used to store excess energy from renewable energy plants. Within this context, proton exchange membrane-electrolyzer and -fuel cells represent integral parts of this value chain, as they are responsible for hydrogen production and its reconversion to electricity. Both technologies have in common that they need a catalyst coated membrane (CCM) to enable the electrochemical conversion. Since nowadays electrolyzer and fuel cell production is still characterized by small-scale production processes, suitable large-scale production lines will be necessary for the market ramp-up. To address these challenges, a novel coating process to produce CCMs is proposed by using a re-coatable transfer belt at which the catalyst ink is coated and dried first. Afterwards, the catalyst ink is transferred onto the membrane by applying a hot-pressing process. Within the presented research, the hot-pressing process is focussed and assessed for the proposed concept. Therefore, the upstream production processes, such as catalyst ink production, coating and drying are described. A design of experiments is then conducted to investigate the applied process parameters within the hot-pressing process and optimized parameters are analysed. Afterwards, re-coating the transfer belt is tested, and the long-term usability of the employed belt is assessed by focussing structural changes.

**Keywords**

Electrolyzer Production; Fuel Cell Production; Catalyst Coated Membrane; Decal coating; Roll-to-roll-production; Industrialization

## 1. Introduction

Industrial production of electrolyzers and fuel cells is still characterised by manufactory production, which is why their production is associated with high costs. To contribute to the market ramp-up of the electrolyzer and the fuel cell, the optimisation of CCM production represents a lever. The CCM is the component where the electrochemical reactions take place. There is cost potential in CCM production due to expensive materials on the one hand, and on the other hand, higher production speeds with consistent quality must be achieved to be able to serve the projected volumes. To address these challenges, an alternative coating process for the membrane of an electrolyzer and a fuel cell is proposed and validated within individual tests, whereby the fuel cell is used as a use case in the context of this paper. The overall objective is to be able to draw conclusions about the development process of the production equipment within the framework of preliminary tests and thus to derive measures for the production equipment development process.

DOI: https://doi.org/10.15488/15242
ISSN: 2701-6277

## 2. Properties and production of catalyst coated membranes

### 2.1 Fundamentals of fuel cell catalyst coated membranes

The proton exchange membrane fuel cell (PEMFC) is an electrochemical energy converter in which the chemical energy of the hydrogen fuel is continuously converted into electrical energy. The individual cell consists of multiple functional layers with the components: Two bipolar half-plates, two gas diffusion layers (GDL), two catalyst layers (CL) and one polymer electrolyte membrane. The CLs applied to the membrane form the catalyst coated membrane (CCM), which is the core component of the PEMFC and the location of the electrochemical reaction. The material properties of the components, the interconnection of membrane and CLs as well as the structure of the CLs have a great influence on the performance and lifetime of the cell and therefore make special demands on the manufacturing steps of the CCM.

The CL applied to the membrane is a heterogeneous porous layer and consists of catalyst particles, carbon support particles and ionomer on the anode and cathode side. Usually, platinum particles (Pt) or platinum alloys with cobalt (PtCo) or nickel (PtNi) are used as catalysts on the cathode side [1], [2]. Since the oxygen reduction reaction of the cathode is considerably slower than the hydrogen oxidation reaction of the anode, the platinum loading of the cathode is higher and its CL thicker than that of the anode [3]. Commercial CCMs typically have a total charge of about 0.4 $mgPt/cm^2$ [4]. The carbon support particles are soot particles with a size of about 50 nm, and Vulcan XC-72 and high-surface-area carbon (HSC), e.g. Ketjenblack [5], are usually used. HSC is less hydrophobic, has a higher internal porosity and a surface area about 4 times larger than Vulcan [6]. Hence, in Vulcan based catalysts most of the Pt particles are on the external surface and in HSC catalysts a large part is in the inner pores [7]. The ionomer is a PFSA polymer and serves as a binder between the particles in the CL and provides electrochemical activity by enabling proton transport to the membrane [8]. The described components catalyst and ionomer together with the reactive gas form the performance-determining triple phase boundary within the CL [9].

### 2.2 Production of catalyst coated membranes

The performance and the described morphology of the CCM is not only dependent on the material selection and composition of the components, but is also influenced by the manufacturing processes, e.g., mixing, coating and drying. The production strategies are differentiated by the substrate on which the ink is applied and dried. In the CCM-based approach, a distinction can be made between direct and indirect coating of the membrane. With direct coating, the ink is applied directly to the membrane, but swelling of the membrane by the water and solvent in the ink is problematic. In indirect coating, the ink is applied to a carrier film, also called decal film, and dried afterwards. The dry CL on the decal film is transferred to the membrane in a further hot-pressing step. [10] Next to the CCM-based approach, coating the GDL is also applicable. The resulting gas diffusion electrode (GDE) is connected to the membrane by hot-pressing; in this case, no CCM is produced. [11] Due to the industrial relevance, the following explanations refer to indirect decal coating. To enable the application of CLs to the decal substrate, a catalyst ink is first prepared in which the CL components Pt nanoparticles supported on carbons (Pt/C) and ionomer are brought into a liquid form. For this purpose, the CL components are mixed in a water/alcohol solution, whereby the exact formulation of the ink determines the microstructure of the catalyst ink. In addition to the formulation, the dispersion process also has an influence on the microstructure. This further determines the macroscopic properties of the ink, such as the rheology, surface tension and stability.[12] With regard to a roll-to-roll process, which is necessary for the further industrialization of fuel cell production, squeegee coating, slot die coating and gravure printing are particularly suitable as coating processes, as with these only one thick homogeneous wet film is applied to the substrate. In particular, slot die coating and gravure printing are investigated in the literature for the production of CLs in roll-to-roll production. [13], [14], [15], [16] In the following drying process, the solvent evaporates from the wet layer of the CL and the morphology of the dry CL is formed.

The evaporation rate of the solvent in particular influences the drying process, with temperatures between 40 °C and 80 °C often being used. [17], [18] The dry CL is then transferred from the decal film to the membrane by applying increased pressure and temperature. The aim is to achieve the highest possible transfer rate from the decal to the membrane and a good bonding between the CL and the membrane. Most publications consider the discontinuous case of a decal transfer in a hot press in batches with the process parameters pressure, temperature, and time. Only the publications by MEHMOOD ET AL. and FRÖHLICH consider the decal transfer as a continuous process with a roller press or calender, using the process parameters of line pressure, temperature and line speed as characterising variables. [11], [19], [20], [21]

## 3. Introduction to the novel process and objective

### 3.1 Description of the novel coating process

The innovative coating process is based on the traditional decal process that is described above. The aim is to save material costs compared to the reference process for the decal material that is used once and then disposed of, and to eliminate the external transfer process, which takes place in an additional process step, and consequently to realise a compact design. The key innovation is a re-coatable, continuous woven and jointless transfer belt. The transfer belt serves as a decal substrate, similar to the decal process, but is directly recoated after the transfer process and runs repeatedly through the entire production process.

The transfer belt passes through the coating, drying, transfer and reuse steps repeatedly. The coating is carried out by a slot die, whereby the substrate is supported by a precision roller and the slot die can be moved to a short distance from the substrate. The catalyst ink is applied to the transfer belt in a homogeneous wet film. After coating, the coated transfer belt passes the drying process. In order to achieve the most compact system design possible and to keep the length of the transfer belt short, infrared drying is used instead of a convection dryer. Compared to convection drying, infrared drying is compared by a much higher heat transfer capacity. Thus, a higher amount of energy can be transferred to the substrate in a shorter time and at lower temperatures. In addition, the infrared radiation diffuses deep into the substrate and the solvents evaporate quickly and effectively.[22] Thus, drying via infrared requires less space compared to convection drying [23]. After drying, the transfer belt passes through the transfer step, in which the transfer belt coated on one side is fed into the calender via a roller. A second roller feeds the membrane. By adjusting the rollers to each other, the necessary line load for the transfer is applied. Additionally, tempering of both rollers ensures the required temperature input for the transfer process. Finally, the transfer belt is guided out of the calender and undergoes the described process again until it is necessary to replace the transfer belt. The one-sided coated membrane is wound up after the transfer, turned and coated on the uncoated side with adapted process parameters, since the anode and cathode of a fuel cell differ from each other, particularly regarding the platinum loading, and optionally also about the used catalyst types.

### 3.2 Objective

To evaluate the proposed coating process, it is necessary to assess both the technical and economic feasibility of the concept. Hence, a preliminary validation is carried out, whereby the focus in this paper is placed on the technical feasibility. After reviewing the process described above, several questions arise that need to be considered in order to be able to make a statement regarding the technical feasibility:

1) How is the coatability of the circulating transfer belt and can a sufficient drying process be conducted?

2) Which process parameters (line pressure, temperature, and line speed) should be applied to realise the highest possible transfer rate within a continuous production?

3) Which impact does a continuous utilization of the transfer belt has onto the produced CCM and onto the transfer belt itself?

As only the technical feasibility of the process itself is to be investigated, convection drying is used for the drying process, which differs from the described infrared dryer. The investigation of infrared drying will be described in a separate document in the future.

## 4. Experimental to assess the technical feasibility of the novel coating process

### 4.1 Assessment of the coatability of the transfer belt

The aim of the investigations is to prove the coatability of the transfer belt with the aim of a defect-free dry dummy CL on the transfer belt. The aim is to achieve the highest possible dry film thickness and carbon loading to simulate cathode layers. For ink production, VULCAN® XC72-R Carbon Black from Carbot is dispersed with ionomer dispersion Aquivion® D83-24B from Solvay S.A., as well as the alcoholic solvent 2-propanol from neoFroxx GmbH or 1-propanol ROTIPURAN® ≥ 99.5% from Carl Roth GmbH together with distilled water. The dispersion is carried out in an ultrasonic bath of the type of Emmi-30HC from Emag AG or by a dissolver of the type DISPERMAT LC75 with a dissolver disc with a diameter of 30 mm from VMA-Getzmann GmbH. A transfer belt made of PTFE-coated glass fibre mesh of the type Fiberflon® 216.13 with a thickness of 125 µm from Fiberflon GmbH is coated by squeegee coating. The coating is applied with an automatic film applicator type ZAA 2600 and squeegee type ZUA 2000 with a width of 220 mm from Zehntner GmbH Testing Instruments. Drying is carried out either at room temperature, on a heating plate of the film applicator or in a heating and drying oven with natural convection of the type of ED 240 from Binder GmbH. The coatability is investigated by iterative layer optimisation with the ink formulations from Table 1. The solids content includes the Vulcan and the dry ionomer.

Table 1: Ink compositions to assess the coatability

| Nr. | Ionomer/Carbon (I/C) [wt.%] | Solvent | Solids content [wt.%] | Solvent/$H_20$ [wt.%] |
|---|---|---|---|---|
| R1 | 1.13 | 2-Propanol | 13.17 | 1.358 |
| R2 | 1.13 | 2-Propanol | 20 | 1.358 |
| R3 | 0.7 | 1-Propanol | 12.75 | 3 |
| R4 | 1 | 2-Propanol | 13 | 3.227 |

### 4.2 Assessment of the transfer rate

A GK 300 L laboratory calender from Saueressig is used for the roll-to-roll transfer. In the test set-up, both rolls are heated. The one-sided transfer of a CL onto the membrane is investigated analogous to the described system concept. In the test set-up, roll-to-roll delamination is carried out with a pretension of 1.42 N/cm and a steep peel angle. The used membrane is a fumapem® FS-715-RFS from Fumatech BWT GmbH. It is a PFSA cation exchange membrane in $H^+$-form with reinforcement with a thickness of 13 – 17 µm. The aim of the investigations is to determine a suitable process window of the transfer, which is why a two-stage, full-factorial experimental design with the three factors temperature, line load and line speed was chosen.

The target variable to be investigated is the transfer rate, i.e., the proportion of CL transferred from the transfer belt to the membrane. Table 2 summarises the selected factor stages.

Table 2: Factor stages of the DoE to investigate the process window of the transfer

| Parameter | Lower value | Upper value |
|---|---|---|
| Temperature (T) [°C] | 150 | 180 |
| Line load (Q) [N/mm] | 22 | 57 |
| Line speed (V) [m/min] | 0.5 | 2 |

A defined coating area of the dummy CL of 220 x 70 (W x L) mm is produced on transfer belt sheets with the dimensions 290 x 200 (W x L) mm. In the transfer, a layer of coated transfer belt, membrane, and another transfer belt, to protect the membrane from the calender rollers, is fed through the calender. The transfer rate is then determined using an optical process by applying a photo evaluation and a Matlab script.

### 4.3 Assessment of the re-coatability of the transfer belt

For the re-coating experiments, one sheet of the transfer belt is cyclically coated, and the layer is transferred to the membrane in the calender transfer. The coated area of the transfer belt is not cleaned in between the cycles to investigate to what extent cleaning is required for the equipment concept. A total of 15 cycles are performed. For each cycle, the transfer rate is determined and used as a criterion for re-coatability. T = 180 °C, V = 0.5 m/min and Q = 57 N/mm are used as transfer parameters, as the best transfer was determined for these in the previous investigations. Formulation R4 with an I/C = 1 is used for the coating. After completion of the repeat tests, the surface of the transfer belt is examined regarding changes. In addition, the mechanical stability and expected service life of the transfer belt are investigated by cyclic calendaring, since the highest thermal and mechanical stress is exerted in the calendering step. For this purpose, a transfer belt sheet is calendered 50 times. Therefore, two different parameter sets (Q = 57 N/mm, T = 180 °C, V = 0.5 m/min and Q = 22 N/mm, T = 180 °C, V = 0.5 m/min) are examined with one sheet each. The basis weight and thickness distribution of the transfer belt are used as criteria for evaluating potential material changes due to the mechanical impact in the transfer belt. To quantify these changes, the assessment of the basis weight and thickness distribution was examined before and after calendering.

## 5. Results

### 5.1 Coatability of the transfer belt

First, the dispersing process is carried out and the viscosity of the catalyst inks produced is examined with a rheometer. Basically, it is recognised that the ionomer in the catalyst ink swells and consequently leads to an increase in viscosity. The swelling behaviour and the associated increase in viscosity is generally dependent on the equivalent weight (EW) of the ionomer, the temperature and time. Stronger swelling behaviour is observed for lower EWs, higher temperatures and longer durations. In addition depending on the dispersion method, agglomerates of different sizes are formed, which influence the subsequent ink application on the substrate. Furthermore, solvent evaporation leads to the fact that the processability of the ink is no longer given if the dispersion time is too long. After the catalyst ink has been applied to the substrate and subsequently dried, a correlation between crack formation and squeegee height or wet film thickness can be identified. For example, while significant cracking can be observed for formulation R1 with a squeegee height of 200 µm, only small surface cracks occur with a squeegee height of 100 µm. In contrast, crack-free layers can be produced with formulation R3 up to 150 µm, which can be attributed to the use of 1-propanol as a solvent. The carbon loading produced here is 0.75 mg/cm$^2$. With formulation R4, layer

thicknesses of up to 100 µm can be produced without defects and with carbon loadings of 0.52 mg/cm$^2$. In addition to the wet film thickness, the solids content is identified as a further influencing factor on the film quality and thus in particular on crack formation. Solids contents that are too high cannot be processed with the squeegee coating. Thus, for recipe R2 with a solids content of 20 wt.%, a crack-free layer cannot be produced even with squeegee heights of 100 µm, whereas this is possible for the other recipes. Furthermore, the subsequent drying also influences the layer quality. After drying at room temperature of approximately 23 °C, the dry CL of an ink of formulation R4 exhibits a stubborn crack structure with crack widths of 40 µm and clod formation. In contrast, an identical comparison sample dried in a heating cabinet at 90 °C shows no cracks. This effect is also observed in the comparison of drying at room temperature and drying on the hot plate at 85 °C, as well as for formulations R1 and R2. Higher drying temperatures therefore seem to reduce cracking for this system, as controlled evaporation of solvent and water is made possible. Taking the described effects into account, a defect-free layer can be produced on the transfer belt, which is used for the transfer rate investigation.

### 5.2 Transfer rate

The corresponding process windows that characterize the transfer process are shown in Figure 1. From the left diagram, the effective relationship of the factors temperature and line load on the transfer rate can be derived, while the speed is maintained. Thus, the transfer rate can be significantly increased to higher temperatures and line loads. For low values (T = 155 °C and Q = 30 N/mm), only a low transfer rate < 40 % is achieved. When increasing these values (T >175 °C and Q > 47 N/mm), transfer rates > 90 % can be realized. This also shows the somewhat stronger effect of temperature on the transfer rate compared to the line load. The dependence of speed and line load is shown in the middle of Figure 1, where the holding value is assumed to be T = 165 °C. The positive influence of the line load on the transfer rate can also be seen, while at the same time the transfer rate decreases with increasing speed. Due to the steeper course of the effective surfaces, it can also be seen that the line load has a higher influence on the transfer rate than the speed. For a given Q = 57 N/mm, this results in a wide speed range of 0.5 – 2 m/min at which a transfer rate > 80 % can be achieved, which is very positive for the economic efficiency of the process.

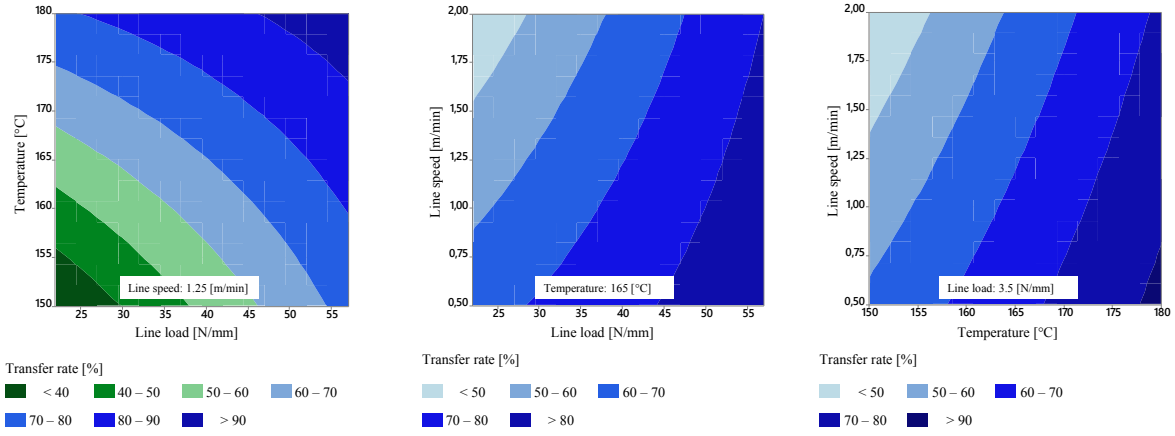


Figure 1: Evaluation of the transfer rates through process windows

The process window as a function of speed and temperature at constant line load (Figure 1, right) is analogous to the one in the middle, but the effective surfaces are even steeper, which on the one hand underlines the stronger influence of the temperature on the transfer rate compared to the line load and on the other hand shows the significantly stronger influence of the temperature compared to the speed. For a selected temperature, this therefore results in a larger speed range with the same transfer rate. Thus, at high

temperatures, high transfer rates can also be achieved at high speeds. If T = 180 °C is chosen, a transfer rate > 90 % can be achieved up to a speed of 0.75 m/min. Accordingly, it can be concluded against the background of the examined transfer rate that the described concept can be operated with economic parameters. By having a more profound look onto the steepness and formation of the shown diagrams in Figure 1, the impact of the three parameters can be ranked. The temperature has the greatest influence on the transfer rate, line load the second greatest and speed the third greatest.

### 5.3 Re-coatability of the transfer belt

The regression line in Figure 2 (left) clearly shows the decreasing trend of the transfer rate. In addition to the decreasing transfer rate, a greater spread of the transfer rate of directly sequential runs can also be observed for the increasing reuse. Accordingly, the process stability of the transfer also decreases with increasing reuse. In addition, punctual residues of the CL remain on the surface of the substrate, which are transferred cyclically to the membrane. This leads to a heterogeneous layer pattern on the membrane. In addition, with the number of repetitions, an increasing adhesion can be seen during delamination, which eventually leads to a less controlled and more abrupt process. This can be explained by residues of ionomer on the transfer belt, from which veils can be seen on the substrate. The described veils ultimately cause the surface energy of the substrate to increase to > 40 mN/m in some cases, drastically limiting adhesion with the catalyst ink. However, cleaning the transfer belt with isopropanol leads to the surface being cleaned in such a way that the original state is restored.

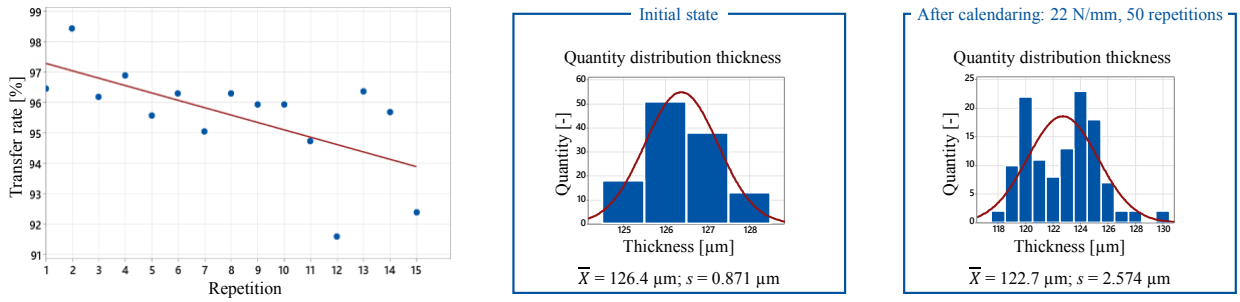


Figure 2: Performance of the re-coating experiment and assessment of the mechanical stability of the transfer belt

In addition to the residues remaining on the transfer belt, an increasing deformation of the transfer belt can be observed with the runs. The mean value of the thickness in the initial state is 126.4 µm. With a standard deviation of 0.871 µm, the spread is low, the measured values scatter between 125 and 128 µm. The frequency distribution follows that of a normal distribution, manufacturing-related systematic inhomogeneities can therefore not be detected and not observed in the surface diagram (Figure 2, centre). Subsequently, the repeat tests in the calender follow, whereby a deformation of the transfer belt can already be seen after 25 repetitions. Thus, starting from the centre towards the outer edges, wave formation occurs. After 50 repetitions, the wave formation is already so pronounced that coating would no longer make sense. The fact that the deformation starts from the centre is most likely due to the inhomogeneous pressure distribution across the width of the calender. Thus, the centre is compressed more than the edge zone, which causes the deformation. Furthermore, an increasing deformation can be seen in the image plane, this is the side with which the transfer belt is inserted into the calender. The larger deformation can be explained by start-up effects. Frequent start-up of the belt should therefore be avoided for the equipment concept. The thickness distribution after the 50 repetitions is shown in Figure 2, right. The mean value of the thickness is reduced to 122.7 µm and the standard deviation is increased to 2.574 µm resulting in a more heterogeneous belt structure.

## 6. Conclusion

In this paper, an alternative coating concept is evaluated regarding its technical feasibility. For this purpose, three questions were raised concerning the coatability, the process parameters of coating transfer and the reusability of a transfer belt. The criterion used for the coatability of the transfer belt is to be able to produce a defect-free, homogeneous, and dry CL on the transfer belt. In this context, not only the wettability in the coating, but also in particular the wettability and adhesion between ink and transfer belt in the drying process turns out to be particularly relevant. The main influencing factors here are the wet film thickness, the water-to-alcohol ratio of the ink, solids content, ink production and the drying temperature. However, overall, crack-free layers with dummy material and sufficient basis weight corresponding to that of a cathode layer on the transfer belt could be produced with a suitable ink formulation and drying parameters. In general, high transfer rates could be achieved in a one-sided roll-to-roll transfer analogous to the planned system concept. A higher line load and temperature as well as a lower speed increase the transfer rate. During the tests, an inhomogeneous pressure distribution of the calender was determined, with a strong pressure drop towards the roll edges, which is why no more transfer could take place in the edge zone. With an edge zone correction to eliminate these inhomogeneities, a transfer rate of > 99.99 % can be achieved with the parameters Q = 57 N/mm and T = 180 °C at V = 2 m/min. Hence, it was possible to prove line speeds that are a factor of 20 faster than what is known in the literature. The technical feasibility of the roll-to-roll transfer with the transfer belt is thus assessed as fulfilled. According to the results on the reuse of the transfer belt, a decreasing transfer rate can be observed with an increasing number of reuses. This is accompanied by an increasing dispersion of the transfer rate, which means a decreasing process stability. The reason for this can be identified as ionomer that is remaining on the transfer belt. These residues lead to increasing adhesion between CL and transfer belt and thus to a more difficult delamination. Furthermore, a partial transfer of the ionomer veil, which accumulates on the transfer belt surface, to the CCM takes place. This then covers the surface of the CCM, which will negatively influence the mass transfer of the reactants into the CL during cell operation. In addition, the mechanical impact of the calender leads to deformations after frequent reuse of the substrate. Accordingly, the results of reusing the transfer belt show further potentials that contribute to the optimization of the proposed process. Thus, on the one hand, the delamination behaviour of the CL must be optimized, which must be homogeneous even after several cycles. In addition, the equipment design should be rethought to the extent that cleaning of the transfer belt is necessary. To further answer these questions, the presented findings can be used, as the correlation between ink composition and layer production was studied. Furthermore, the transfer properties were extensively investigated and quantified.


### Acknowledgement

This research was funded by Federal Ministry for Economic Affairs and Climate Action, Germany grant number 03EN5013A-FCPP.


### References


[1] Borup, R.L., Kusoglu, A., Neyerlin, K.C., Mukundan, R., Ahluwalia, R.K., Cullen, D.A., More, K.L., Weber, A.Z., Myers, D.J., 2020. Recent developments in catalyst-related PEM fuel cell durability. Current Opinion in Electrochemistry 21, 192–200.

[2] Xing, W., 2008. Catalyst Layer Composition Optimization, in: Zhang, J. (Ed.), PEM fuel cell electrocatalysts and catalyst layers. Fundamentals and applications. Springer, London, Heidelberg, pp. 1003–1040.

[3] Dicks, A., Rand, D.A.J., 2018. Fuel cell systems explained, Third edition ed. John Wiley & Sons Inc, Hoboken, New Jersey, 460 pp.

[4] Xie, M., Chu, T., Wang, T., Wan, K., Yang, D., Li, B., Ming, P., Zhang, C., 2021. Preparation, Performance and Challenges of Catalyst Layer for Proton Exchange Membrane Fuel Cell. Membranes 11 (11).

[5] Chowdhury, A., Darling, R.M., Radke, C.J., Weber, A.Z., 2019. Modeling Water Uptake and Pt Utilization in High Surface Area Carbon. ECS Trans. 92 (8), 247–259.

[6] Padgett, E., Andrejevic, N., Liu, Z., Kongkanand, A., Gu, W., Moriyama, K., Jiang, Y., Kumaraguru, S., Moylan, T.E., Kukreja, R., Muller, D.A., 2018. Editors' Choice—Connecting Fuel Cell Catalyst Nanostructure and Accessibility Using Quantitative Cryo-STEM Tomography. J. Electrochem. Soc. 165 (3), F173-F180.

[7] Berlinger, S.A., Garg, S., Weber, A.Z., 2021. Multicomponent, multiphase interactions in fuel-cell inks. Current Opinion in Electrochemistry 29, 100744.

[8] Holdcroft, S., 2014. Fuel Cell Catalyst Layers: A Polymer Science Perspective. Chem. Mater. 26 (1), 381–393.

[9] Khandavalli, S., Park, J.H., Kariuki, N.N., Myers, D.J., Stickel, J.J., Hurst, K., Neyerlin, K.C., Ulsh, M., Mauger, S.A., 2018. Rheological Investigation on the Microstructure of Fuel Cell Catalyst Inks. ACS applied materials & interfaces 10 (50), 43610–43622.

[10] Wilson, M.S., Gottesfeld, S., 1992. High Performance Catalyzed Membranes of Ultra-low Pt Loadings for Polymer Electrolyte Fuel Cells. J. Electrochem. Soc. 139 (2), L28-L30.

[11] Frölich, K., 2015. Der Decal-Prozess zur Herstellung katalysatorbeschichteter Membranen für PEM-Brennstoffzellen. Dissertation, Karlsruher Institut für Technologie (KIT).

[12] Liu, H., Ney, L., Zamel, N., Li, X., 2022. Effect of Catalyst Ink and Formation Process on the Multiscale Structure of Catalyst Layers in PEM Fuel Cells. Applied Sciences 12 (8), 3776.

[13] Siegel, F., 2015. Tiefdruckverfahren zur Herstellung von Katalysatorschichten für (PEM) Brennstoffzellen, Chemnitz.

[14] Mauger, S.A., Wang, M., Medina, S., Pylypenko, S., Ulsh, M., 2019. Influence of Coating Method on Performance of Roll-to-Roll Coated PEM Fuel Cell Catalyst Layers. https://www.nrel.gov/docs/fy20osti/77815.pdf. Accessed 15 February 2023.

[15] Burdzik, A., Stähler, M., Friedrich, I., Carmo, M., Stolten, D., 2018. Homogeneity analysis of square meter-sized electrodes for PEM electrolysis and PEM fuel cells. J Coat Technol Res 15 (6), 1423–1432.

[16] Liu, P., Li, B., Yang, D., Zhang, C., Ming, P., 2023. New insights on the agglomeration and sedimentation behaviours of catalyst ink of proton exchange membrane fuel cells affected by ionomers concentration. Journal of Power Sources 556, 232427.

[17] Suzuki, T., Tanaka, H., Hayase, M., Tsushima, S., Hirai, S., 2016. Investigation of porous structure formation of catalyst layers for proton exchange membrane fuel cells and their effect on cell performance. International Journal of Hydrogen Energy 41 (44), 20326–20335.

[18] Mauger, S.A., Wang, M., Cetinbas, F.C., Dzara, M.J., Park, J., Myers, D.J., Ahluwalia, R.K., Pylypenko, S., Hu, L., Litster, S., Neyerlin, K.C., Ulsh, M., 2021. Development of high-performance roll-to-roll-coated gas-diffusion-electrode-based fuel cells. Journal of Power Sources 506, 230039.

[19] Mehmood, A., Ha, H.Y., 2013. Parametric investigation of a high-yield decal technique to fabricate membrane electrode assemblies for direct methanol fuel cells. International Journal of Hydrogen Energy 38 (28), 12427–12437.

[20] Mehmood, A., Ha, H.Y., 2012. An efficient decal transfer method using a roll-press to fabricate membrane electrode assemblies for direct methanol fuel cells. International Journal of Hydrogen Energy 37 (23), 18463–18470.

[21] Gatto, I., Saccà, A., Baglio, V., Aricò, A.S., Oldani, C., Merlo, L., Carbone, A., 2019. Evaluation of hot pressing parameters on the electrochemical performance of MEAs based on Aquivion® PFSA membranes. Journal of Energy Chemistry 35, 168–173.

[22] Lambda Technology. Technologie. https://lambdatechnology.com/wellenlaenge-physik/. Accessed 23 April 2023.

[23] Wöll, J., 2018. Platz, Zeit und Energie sparen. J Oberfl Techn 58 (1), 14–17.

## Biography

***Achim Kampker*** *(*1976) is head of the chair "Production Engineering of E-Mobility Components" (PEM) of RWTH Aachen University and known for his co-development of the "StreetScooter" electric vehicle. Kampker also acts as member of the executive board of the "Fraunhofer Research Institution for Battery Cell Production FFB" in Münster. He is involved in various expert groups of the federal and state governments.*

***Heiner Hans Heimes*** *(*1983) studied mechanical engineering with a focus on production engineering at RWTH Aachen University. From 2015 to 2019, he was head of the Electromobility Laboratory (eLab) of RWTH Aachen University. From March 2019 to 2023, he was PEM's Executive Chief Engineer before being appointed Professor.*

***Mario Kehrer*** *(*1990) studied electrical engineering and information technology at Karlsruhe Institute of Technology (KIT). He joined the chair "Production Engineering of E-Mobility Components" (PEM) of RWTH Aachen University in 2017, where he became chief engineer of the Fuel Cell and Electrification Engineering division in 2021.*

***Sebastian Hagedorn*** *(*1992) studied mechanical engineering with a focus on production engineering at RWTH Aachen University. After joining the chair "Production Engineering of E-Mobility Components" (PEM) of RWTH Aachen University in 2019, Hagedorn became the leader of the Fuel Cell group in 2021.*

***Niels Hinrichs*** *(*1996) is research assistant at the Chair of Production Engineering of E-Mobility Components (PEM) at RWTH Aachen University. He studied mechanical engineering with a focus on energy and process engineering at Ruhr-University Bochum.*

***Philip Heyer*** *(*1994) studied industrial engineering with a focus on production engineering at RWTH Aachen University. Heyer worked as a research assistant and completed master's degree with a master thesis at the Chair of Production Engineering of E-Mobility Components (PEM) at RWTH Aachen University.*